Available online at www.sciencedirect.com

SciVerse ScienceDirect

Ceramics International 38 (2012) 4357–4361

CERAMICS INTERNATIONAL

www.elsevier.com/locate/ceramint

Short communication

Thermal conductivity of $(Hf_{1-x}Zr_x)_6Ta_2O_{17}$ ($x = 0$, 0.1, 0.3 and 0.5) ceramics

Miao Li *, Qiang Xu, Lu Wang

School of Materials Science and Engineering, Beijing Institute of Technology, Beijing 100081, PR China

Received 19 December 2011; received in revised form 30 December 2011; accepted 31 December 2011
Available online 10 January 2012

Abstract

$(Hf_{1-x}Zr_x)_6Ta_2O_{17}$ ($x = 0$, 0.1, 0.3 and 0.5) ceramic powders were synthesized by conventional solid-state method. The samples of these ceramics were prepared by pressureless sintering process at 1600 °C for 8 h in air. X-ray diffraction characterization indicated that all samples were single phase with orthorhombic structure. The thermal diffusivities of the samples from 200 °C to 1000 °C were characterized by laser flash diffusivity measurement. The thermal conductivities of $(Hf_{1-x}Zr_x)_6Ta_2O_{17}$ decreased with the increase of zirconium content x. Thermal conductivity of $(Hf_{0.5}Zr_{0.5})_6Ta_2O_{17}$ was about 2.75 W/m K which was comparable with that of dense partially yttria-stabilized zirconia (~2.5 W/m K).

Keywords: C. Thermal conductivity; $(Hf_{1-x}Zr_x)_6Ta_2O_{17}$; Zirconium doped

1. Introduction

Thermal barrier coatings (TBCs) are used in gas turbines to protect alloy components from high temperature. The current state-of-art of TBCs in commercial use is 6–8 wt.% partially yttria-stabilized zirconia (6–8YSZ) with high melting point and low thermal conductivity. When the combustion-chamber temperature is up to 1200 °C, YSZ layers experience phase transformation which result in the failure of TBCs [1–3]. Therefore, oxide ceramics with high melting point, good phase stability and low thermal conductivity have been developed as candidate materials for future TBCs [4,5].

The melting point of oxide ceramic is proportional to intensity of chemical bonds [6]. Therefore, it can be presumed that $Hf_6Ta_2O_{17}$ has comparatively high melting point. $Hf_6Ta_2O_{17}$ has only a kind of phase structure in the open reports [7], and has no phase transformation from room temperature to 1400 °C in our experiments [8]. $Hf_6Ta_2O_{17}$ maybe has low thermal conductivity because of large molecular weight and complex crystal structure [9]. The minimum of thermal conductivity is expressed by experimental formula [9]:

$$\kappa_{\min} = 0.87 k_B \overline{\Omega}^{-2/3} \left(\frac{E}{\rho}\right)^{1/2} \tag{1}$$

$$\overline{\Omega} = \frac{M}{m\rho N} \tag{2}$$

where $\overline{\Omega}$ is an effective atomic volume, M is the mean atomic mass of the ions in the unit cell, m is the number of ions in the unit cell, ρ is the density, E is Young's modulus, k_B and N_A are Boltzmann's constant and Avagadro's number.

Thermal conductivity is mainly determined by the free path of phonon, and the free path of phonon can be reduced by foreign ions doped. The free path of phonon $\overline{l}$ can be expressed by the following equations [10]:

$$\frac{1}{\overline{l}} = \frac{ca^3\omega^4}{4\pi v^4}\left(\frac{\Delta M}{M}\right)^2 \tag{3}$$

$$\frac{1}{\overline{l}} = \frac{2ca^3\omega^4}{\pi v^4} J^2\gamma^2\left(\frac{\Delta R}{R}\right)^2 \tag{4}$$

where a^3 is the volume per atom, v is the transverse wave speed, ω is the phonon frequency, c is the concentration per atom, J is a constant, γ is the Grüneisen parameter, M and R are the average mass and ionic radius of the host atom, ΔM and ΔR are the differences of mass and ionic radius between the substituted and substituting atoms, respectively. Eqs. (3) and (4) indicate that the mean free path of phonon is proportional to the square of the difference of mass and ionic radius between the substituted and substituting atoms.

Zirconium is chosen as substituting atom because it has same electrovalence and similar ionic radius with hafnium.

* Corresponding author. Tel.: +86 13671365491; fax: +86 68911144 869.
E-mail address: limiaobit@gmail.com (M. Li).

0272-8842/$36.00 © 2012 Published by Elsevier Ltd and Techna Group S.r.l.
doi:10.1016/j.ceramint.2011.12.080

According to Eqs. (3) and (4), it is known that the mean free path of phonon in $(Hf_{1-x}Zr_x)_6Ta_2O_{17}$ lattice decreases with the increase of zirconium content x. The mean free path of phonon is shortest when x is 0.5. Therefore, it can be presumed that $(Hf_{0.5}Zr_{0.5})_6Ta_2O_{17}$ has the lowest thermal conductivity.

In the present research, $(Hf_{1-x}Zr_x)_6Ta_2O_{17}$ ($x = 0$, 0.1, 0.3 and 0.5) ceramic powders were synthesized by solid-state method. The thermal conductivities of these ceramics were investigated and the effect of zirconium doped on thermal conductivity was analyzed.

2. Materials and methods

2.1. Starting materials

The starting materials are Ta_2O_5 with purity of 99.9%, HfO_2 of 99.9%, and ZrO_2 of 99.9%.

2.2. Preparation of ceramic powders and sintered samples

The starting materials were weighed in the stoichiometric proportions, and mixed by ball-milling in ethanol with zirconia balls for 6 h. The mixtures were dried, molded, cold pressed isostatically at 200 MPa, and then sintered at 1600 °C for 8 h in air by LHT04/17 high-temperature sintered furnace (NABERTHERM Co. Ltd., Germany). The mixed powders were annealed at 1600 °C for 8 h in air.

2.3. Experimental methods

The phase structures of the sintered samples and the annealed powders were characterized by X'Pert PRD MPD instrument (PANalytical Co. Ltd., Netherlands) with Cu Kα radiation (0.1542 nm) at a scanning rate of 4°/min. The surface morphology of the sintered samples was investigated by S-4800 scanning electron microscopy (HITACHI Ltd., Japan). After polished, the samples were annealed at 1500 °C for 1 h in air. The crystal morphology of the annealed samples was investigated. Densities (ρ) of the sintered samples were obtained by the Archimedes method with an immersion medium of distilled water.

The thermal diffusivities (λ) of the sintered samples were measured by Flashline5000 system (Anter Co. Ltd., USA) at the temperature range from 200 °C to 1000 °C in an argon atmosphere. The error of thermal diffusivity is ±5%. The sample dimensions for thermal diffusivity were 12.7 mm in diameter and 1 mm in thickness. Before the measurement of thermal diffusivity, both the front and back faces of the samples were coated with a thin layer of graphite. These coatings were done to prevent direct transmission of laser beam through the translucent samples.

The thermal conductivities (κ) of the sintered samples were given by the following equation with thermal diffusivity (λ), density (ρ) and specific heat capacity (C_p):

$$\kappa = \lambda \rho C_p \tag{5}$$

Because the sintered sample is not fully dense (100%), the measured value of thermal conductivity is modified for the actual data (κ_0) using the following equation [11]:

$$\frac{\kappa}{\kappa_0} = \frac{1 - 4\phi}{3} \tag{6}$$

where ϕ is the fractional porosity of the sintered sample.

The specific heat capacities (C_{pi}) of HfO_2, ZrO_2 and Ta_2O_5 from 200 °C to 1000 °C can be fitted as the following equation [12]:

$$C_{pi} = a + b \times 10^{-3}T + c \times 10^{5}T^{-2} \tag{7}$$

where T is temperature, a, b, c are the constants of oxides.

The approximate values of specific heat capacities (C_p) of $(Hf_{1-x}Zr_x)_6Ta_2O_{17}$ at different temperatures were calculated by the addition of the specific heat capacities of HfO_2, ZrO_2 and Ta_2O_5 as the following equation [13]:

$$C_p = pC_{p1} + qC_{p2} + rC_{p3} - \Delta G \tag{8}$$

where p, q, r are the mole amounts of HfO_2, ZrO_2 and Ta_2O_5 in one mole $(Hf_{1-x}Zr_x)_6Ta_2O_{17}$, C_{p1}, C_{p2}, C_{p3} are the specific heat capacities of HfO_2, ZrO_2 and Ta_2O_5, ΔG is the change of Gibbs free energy in solid-state reaction process. ΔG is neglected because it is small.

3. Results and discussion

3.1. Phase structure

The XRD diffraction patterns of the sintered samples are presented in Fig. 1. All samples are of single phase in orthorhombic symmetry. The diffraction degrees (2θ) of the strongest diffraction peaks of the annealed powders are shown in Table 1. The diffraction degrees (2θ) have been modified by pure Si powder. As zirconium content x is increasing, the degrees of the peaks (2θ) decrease. According to Bragg equation, it is known that the lattices of $(Hf_{1-x}Zr_x)_6Ta_2O_{17}$ expand with the increase of zirconium content x. The ionic

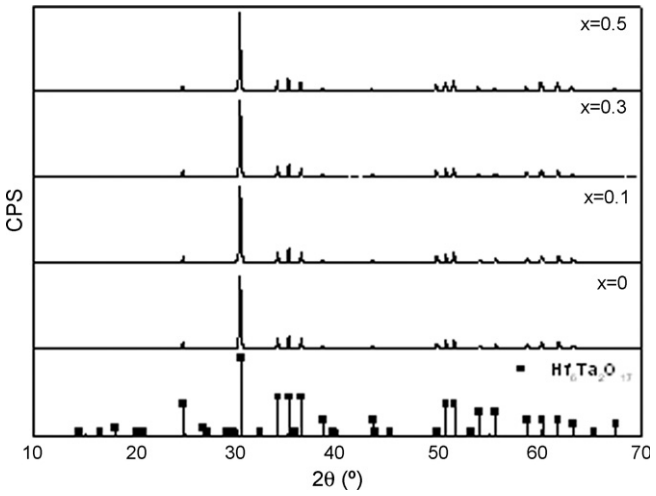

Fig. 1. X-ray diffraction patterns of $(Hf_{1-x}Zr_x)_6Ta_2O_{17}$ ($x = 0$, 0.1, 0.3 and 0.5) sintered samples.

Table 1
Diffraction degrees (2θ) of the strongest diffraction peaks of $(Hf_{1-x}Zr_x)_6Ta_2O_{17}$ ($x = 0$, 0.1, 0.2, 0.3, 0.4, 0.5) powders.

x	2θ (°)
0	30.7127
0.1	30.6925
0.2	30.6741
0.3	10.6554
0.4	30.6366
0.5	30.6047

radius of Zr^{4+} (0.78 Å in sevenfold coordinated, 0.84 Å in eightfold coordinated) is larger than that of Hf^{4+} (0.76 Å in sevenfold coordinated, 0.83 Å in eightfold coordinated). This results in the expansion of $(Hf_{1-x}Zr_x)_6Ta_2O_{17}$ lattices when Hf^{4+} is substituted by Zr^{4+}.

3.2. Surface morphology and crystal morphology

The surface morphology and crystal morphology of the samples are shown in Figs. 2 and 3. All samples are compact

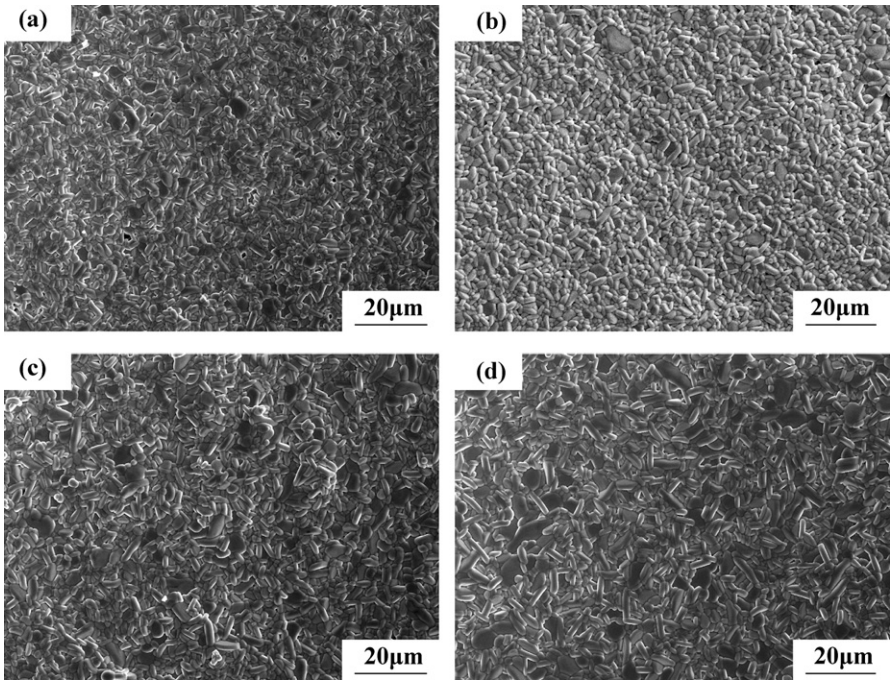

Fig. 2. Surface morphology of $(Hf_{1-x}Zr_x)_6Ta_2O_{17}$ ($x = 0$, 0.1, 0.3 and 0.5) sintered samples ((a) $x = 0$, (b) $x = 0.1$, (c) $x = 0.3$ and (d) $x = 0.5$).

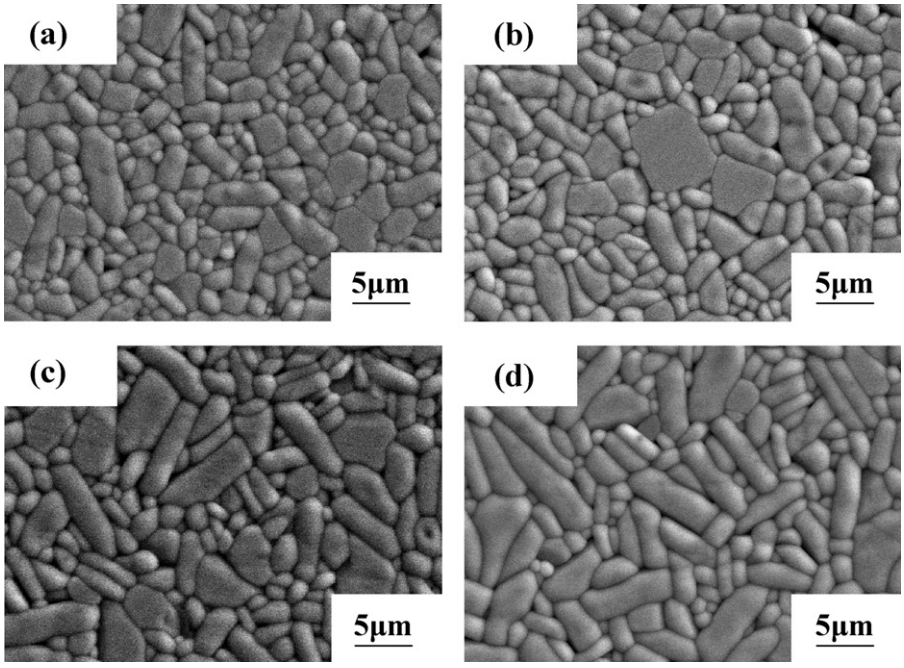

Fig. 3. Crystal morphology of $(Hf_{1-x}Zr_x)_6Ta_2O_{17}$ ($x = 0$, 0.1, 0.3 and 0.5) sintered samples ((a) $x = 0$, (b) $x = 0.1$, (c) $x = 0.3$ and (d) $x = 0.5$).

Table 2
The densities and porosities of $(Hf_{1-x}Zr_x)_6Ta_2O_{17}$ ($x = 0$, 0.1, 0.3 and 0.5) sintered samples.

x	Academic density (g/cm^3)	Actual density (g/cm^3)	Relative density (wt.%)	Porosity (vol.%)
0	10.9524	10.2354	93.45	6.55
0.1	10.5999	10.0494	94.81	5.19
0.3	9.8971	9.4894	95.88	4.12
0.5	9.1936	8.5044	92.50	7.50

and holes are few. The crystal boundaries are clean and no other inter-phases or original oxides exist. Crystals in all samples are anisotropic. Crystal size is about between 1 μm and 5 μm. The densities (ρ) and porosities (ϕ) are shown in Table 2. The academic density and actual density of $(Hf_{1-x}Zr_x)_6Ta_2O_{17}$ samples decrease with the increase of zirconium content x because the mass of zirconium (91.224) is smaller than that of hafnium (178.49).

3.3. Thermal diffusivity and thermal conductivity

The thermal diffusivities (λ) of the sintered samples from 200 °C to 1000 °C are plotted in Fig. 4. The thermal diffusivities of $(Hf_{1-x}Zr_x)_6Ta_2O_{17}$ ($x = 0$, 0.1 and 0.3) samples decrease with the increase of temperature under 600 °C, and then increase at higher temperature. The value of thermal diffusivities at 600 °C is the lowest. The thermal diffusivities of $(Hf_{0.5}Zr_{0.5})_6Ta_2O_{17}$ sample decrease with the increase of temperature continuously. It is because the thermal diffusivities of $(Hf_{1-x}Zr_x)_6Ta_2O_{17}$ were also affected by oxygen vacancies. At 600 °C, a great deal oxygen vacancies appear in $(Hf_{1-x}Zr_x)_6Ta_2O_{17}$ lattice which enhance the phonon scattering and reduce the mean free path of phonon [10,14]. However, the amounts of oxygen vacancies in $(Hf_{1-x}Zr_x)_6Ta_2O_{17}$ lattice are limited, and so the influence of oxygen vacancies are not notable when the temperature is up to 600 °C. The amount of oxygen vacancies decreases as the zirconium content x increases which is observed in the measurement of oxygen ions conductivity. Therefore, the effect of oxygen vacancies on the thermal diffusivity of $(Hf_{0.5}Zr_{0.5})_6Ta_2O_{17}$ is not remarkable as other samples.

Table 3
Specific heat capacities (kJ/kg °C) of $(Hf_{1-x}Zr_x)_6Ta_2O_{17}$ ($x = 0$, 0.1, 0.3 and 0.5) ceramics.

x	T (°C)					
	200	400	600	800	1000	1200
0	580.639	620.027	645.514	666.391	685.310	703.255
0.1	578.140	617.623	643.024	663.764	682.523	700.300
0.3	573.415	613.114	638.160	658.513	676.866	694.396
0.5	569.520	608.604	633.625	653.834	671.918	689.085

The approximate values of specific heat capacities (C_p) of $(Hf_{1-x}Zr_x)_6Ta_2O_{17}$ ($x = 0$, 0.1, 0.3 and 0.5) at different temperature are presented in Table 3. The values of specific heat capacities increase with the increase of temperature and decrease with the increase of zirconium content x. The calculated values are larger than actual values because ΔG is neglected.

The thermal conductivities (κ_0) of $(Hf_{1-x}Zr_x)_6Ta_2O_{17}$ ($x = 0$, 0.1, 0.3 and 0.5) from 200 °C to 1000 °C are plotted in Fig. 5. The thermal conductivities of $(Hf_{1-x}Zr_x)_6Ta_2O_{17}$ decrease with the increase of zirconium content x. $(Hf_{0.5}Zr_{0.5})_6Ta_2O_{17}$ has the lowest thermal conductivity (~2.75 W/m K) which is comparable with that of dense YSZ (~2.5 W/m K) [5]. Thermal conductivity of $(Hf_{1-x}Zr_x)_6Ta_2O_{17}$ is reduced by zirconium doped because the mean free path of phonon is shortened by foreign ions doped. The result is consistent with Eqs. (3) and (4).

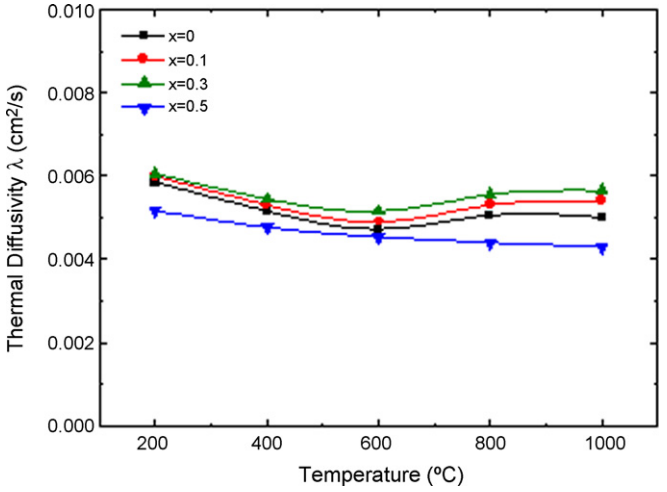

Fig. 4. Thermal diffusivities of $(Hf_{1-x}Zr_x)_6Ta_2O_{17}$ ($x = 0$, 0.1, 0.3 and 0.5) sintered samples from 200 °C to 1000 °C.

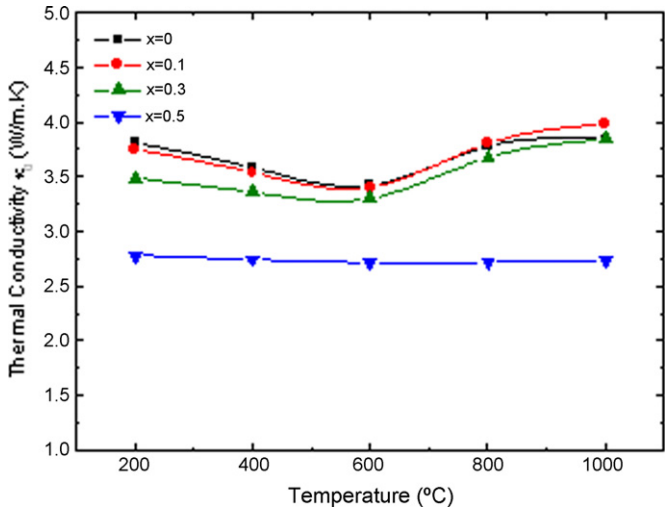

Fig. 5. Thermal conductivities of $(Hf_{1-x}Zr_x)_6Ta_2O_{17}$ ($x = 0$, 0.1, 0.3 and 0.5) from 200 °C to 1000 °C.

4. Conclusions

Single phase $(Hf_{1-x}Zr_x)_6Ta_2O_{17}$ ($x = 0$, 0.1, 0.3 and 0.5) ceramics were synthesized by solid-state method, and the thermal diffusivities of these ceramics were characterized by laser flash method. The thermal conductivities of $(Hf_{1-x}Zr_x)_6Ta_2O_{17}$ ($x = 0$, 0.1, 0.3 and 0.5) were reduced by zirconium doped, because the mean free path of phonon was shortened by foreign ions. The value of the thermal conductivity of $(Hf_{0.5}Zr_{0.5})_6Ta_2O_{17}$ is comparable with that of dense YSZ. It is concluded that these ceramics can be considered as candidate materials for thermal barrier coatings.

Acknowledgments

The author would like to thank Professor Xu Qiang, Professor Wang Lu, Professor Zhu Shizhen, Doctor Liu Ling and National Natural Science Foundation of China.

References

[1] Q. Yu, C. Zhou, H. Zhang, et al., Thermal stability of nanostructured 13wt%Al_2O_3–8wt%Y_2O_3–ZrO_2 thermal barrier coatings, J. Eur. Ceram. Soc. 30 (2010) 889–897.

[2] H. Liu, S. Li, Q. Li, et al., Investigation on the phase stability, sintering and thermal conductivity of Sc_2O_3–Y_2O_3–ZrO_2 for thermal barrier coating application, Mater. Des. 31 (2010) 2972–2977.

[3] Y. Shen, R.M. Leckie, C.G. Levi, et al., Low thermal conductivity without oxygen vacancies in equimolar $YO_{1.5}$ + $TaO_{2.5}$- and $YbO_{1.5}$ + $TaO_{2.5}$-stabilized tetragonal zirconia ceramics, Acta Mater. 58 (2010) 4424–4431.

[4] X.Q. Cao, R. Vassen, D. Stoever, Ceramic materials for thermal barrier coatings, J. Eur. Ceram. Soc. 24 (2004) 1–10.

[5] M.R. Winter, D.R. Clarke, Oxide materials with low thermal conductivity, J. Am. Ceram. Soc. 90 (2) (2007) 533–540.

[6] J. Wang, L. Li, B.J. Campbell, et al., Structure, thermal expansion and transport properties of $BaCe_{1-x}Eu_xO_{3-\delta}$ oxides, J. Mater. Chem. Phys. 86 (2004) 150–155.

[7] International Center of Diffraction Data (2000) 44-0998.

[8] M. Li, Q. Xu, S. Zhu, et al., Preparation and thermal expansion of $Hf_6Ta_2O_{17}$ ceramic, Rare Met. Mater. Eng., in press.

[9] D.R. Clarke, Materials selection guidelines for low thermal conductivity thermal barrier coatings, Surf. Coat. Technol. 163 (2003) 67–74.

[10] P.G. Klemens, Phonon scattering by oxygen vacancies in ceramics, J. Phys. B 263–264 (1999) 102–104.

[11] K.W. Schlichting, N.P. Padture, P.G. Klemens, Thermal conductivity of dense and porous yttria-stabilized zirconia, J. Mater. Sci. 36 (2001) 3003–3010.

[12] P.G. Spencer, Estimation of thermodynamic data for metallurgical applications, Thermochim. Acta 314 (1998) 1–21.

[13] J.D. Leitner, P. Chuchvalec, D. Sedmidubsky, Estimation of heat capacity of solid mixed oxides, Thermochim. Acta 395 (2003) 27–46.

[14] F.L. Madarasz, P.G. Klemens, Reduction of lattice thermal conductivity by point defects at intermediate temperatures, Int. J. Thermophys. 8 (2) (1987) 257–262.